The turbulent kinetic energy budget in the marine atmospheric surface layer

Anna Sjöblom and Ann-Sofi Smedman

Department of Earth Sciences, Meteorology, Uppsala University, Uppsala, Sweden

Received 11 June 2001; revised 18 December 2001; accepted 17 April 2002; published 9 October 2002.

[1] The terms in the turbulent kinetic energy (TKE) budget have been analyzed according to stability, wave age, and wind speed, using long-term measurements over the sea. The measurements were performed at the island Östergarnsholm in the middle of the Baltic Sea. The results show that there is an imbalance between normalized production and normalized dissipation, also in neutral conditions, and that this imbalance depends not only on stability, which has been previously suggested, but also on wave age and wind speed. For small wave ages and high wind speeds, production is larger than dissipation at neutral conditions. For saturated waves and moderate wind speeds, the sea surface resembles a land surface, while for swell and low wind speeds, dissipation strongly exceeds production. The normalized pressure transport becomes significant during swell conditions, and is not balanced by the normalized turbulent transport. ''Inactive'' turbulence, where energy is being brought down to the surface from higher levels, is probably the reason for these high values of the pressure transport. The traditional ''inertial dissipation method,'' where the sum of the transport terms is assumed small and neglected, therefore needs to be corrected for an imbalance between production and dissipation. *INDEX TERMS:* 3339 Meteorology and Atmospheric Dynamics: Ocean/atmosphere interactions (0312, 4504); 3384 Meteorology and Atmospheric Dynamics: Waves and tides; 4247 Oceanography: General: Marine meteorology; 4504 Oceanography: Physical: Air/sea interactions (0312); 4560 Oceanography: Physical: Surface waves and tides (1255); *KEYWORDS:* inertial dissipation method; marine atmospheric boundary layer; swell; turbulent kinetic energy budget; waves

Citation: Sjöblom, A., and A. Smedman, The turbulent kinetic energy budget in the marine atmospheric surface layer, *J. Geophys. Res.*, *107*(C10), 3142, doi:10.1029/2001JC001016, 2002.

1. Introduction

[2] The energy exchange at the surface of the oceans plays a decisive role for the climate of the Earth. In modeling these energy fluxes, it is vital that the physics of the governing processes is correctly understood. Traditionally, results obtained over land are employed. Recent research (for references, see below) has, however, identified processes which depend critically on specific air-sea interaction mechanisms and which are not taken into account in current models. The effects are expected to depend on the wave state, i.e., the degree of wave development, including the effect of swell originating in distant areas.

[3] Most air-sea interaction experiments in the past are either offshore experiments of limited duration and with measurements at only one level or coastal measurements at nearshore sites. In this paper data are analyzed from several years worth of measurements on a small island, Östergarnsholm, in the Baltic Sea. The data include eddy correlation measurements at three levels and wave measurements outside the island. From previous analysis [*Smedman et al.*, 1999, appendix B] it is known that the measured fluxes at approximately 10 m at this site, are likely to be largely representative of deep sea conditions even during gale winds. The present analysis aims at studying the turbulent kinetic energy (TKE) budget in a wide range of conditions. Knowledge of the behavior of each term in the TKE-budget is fundamental for application of the widely used inertial dissipation method.

[4] Several methods for calculating fluxes over the sea are used today. The ''bulk aerodynamical method'' uses only mean meteorological parameters and is probably the most practical method for climatological purposes. The largest uncertainty in this method is the numerical values of the drag coefficients, but there is also a problem to determine a correct wind speed from a moving ship or buoy.

[5] The ''eddy-correlation method'' or ''direct covariance method'' is the most direct way to determine the fluxes since the correlation between fluctuations of measured quantities (for example u and w) can be measured directly, and from that the stress and the heat fluxes can be calculated. A serious problem, however, is that the instruments usually have to be mounted on a buoy or on a ship, and the frequencies of the movement of the buoy or ship are in the same interval as that of the flux itself. Thus it is very difficult to make corrections. The eddy-correlation method is also very sensitive to flow distortion [e.g., *Edson et al.*, 1991].

[6] However, *Anctil et al.* [1994] and *Edson and Fairall* [1998] give examples of measurements on buoys where the

0148-0227/02/2001JC001016

eddy-correlation method is used and where corrections have been successfully applied.

[7] The inertial dissipation method has been used for about 30 years as a method to measure wind stress over the ocean [*Smith et al.*, 1996], but the technique has had a reputation of being very "fragile and exotic," relying on many assumptions and very fragile sensors [*Fairall et al.*, 1990]. Today more robust instruments can be used, and the algorithms have been improved.

[8] During HEXOS main field experiment HEXMAX [e.g., *Katsaros et al.*, 1987; *Smith et al.*, 1992; *DeCosmo et al.*, 1996], a detailed comparison of the inertial dissipation against the eddy correlation method was performed [*Edson et al.*, 1991; *Fairall et al.*, 1990]. The measurements took place on the Dutch offshore platform Meetpost Noordwijk in the North Sea in October and November 1986. The estimates with the inertial dissipation method agreed well with the direct covariance method, and the results gave an uncertainty of 10% for stress, 20% for sensible heat flux, and 25% for latent heat flux [*Fairall et al.*, 1990].

[9] The inertial dissipation method has many advantages: Only measurements in the inertial subrange are needed, and these high-frequency fluctuations can easily be separated from the disturbances caused by the movements of for example a ship. The wind speed needed for the calculations is the apparent wind speed, which is the wind speed actually measured on-board (i.e., the wind speed relative to the moving platform). Explicit measurements of the vertical velocity are in this case avoided. It is also clear that this method is superior to the direct covariance method in regions of severe flow distortion [*Edson et al.*, 1991].

[10] There are, however, disadvantages with the inertial dissipation method. It relies on several assumptions and choices of constants and these need to be further investigated for the method to be reliable under all conditions. It also builds on a correct parameterization of the terms in the TKE-budget.

[11] The energy budget has been quite well analyzed over land [e.g., *Wyngaard and Cote*, 1971; *Högström*, 1990], even if the results sometimes are inconclusive. There have not been as many measurements of the TKE-budget over sea, and there are still a lot of uncertainties regarding the different terms, and whether the results are the same over sea as over land. The problem with earlier measurements over sea is that all terms have not been determined directly, normally only production and dissipation were measured, and not the transport terms [e.g., *Edson and Fairall*, 1998].

[12] The response of the TKE-budget to different wave conditions has not been investigated thoroughly up till now. There are, however, some earlier studies of wave influence on the turbulent structures in the marine atmospheric surface layer. The influence of swell, that is waves traveling faster than the wind, was considered already in the 70s by, for example, *Kitaigorodskii* [1973], *Makova* [1975], *Volkov* [1970], and *Benilov et al.* [1974]. They discussed a "supersmooth" surface and how waves traveling faster than the wind would influence the measurements. How swell actually does influence the turbulence structure of the atmospheric boundary layer has been a controversial question in the last years, but nowadays the influence of swell is more or less accepted [e.g., *Smedman et al.*, 1999]. There is evidence that the influence of swell can reach up to a considerable height [*Makova*,1975; *Drennan et al.*, 1999b; *Smedman et al.*, 1994] in contrast to the influence of growing waves.

[13] During swell conditions, it has been argued that the traditional inertial dissipation method can not be used [e.g., *Donelan et al.*, 1997]. A major problem with the inertial dissipation method is that it is not possible to detect the direction of the flux. It automatically gives a positive value of the total stress (τ) [*Grachev and Fairall*, 2001], which is not always the case in swell conditions.

[14] The current investigation is a study of the TKE-budget using long-term measurements over the Baltic Sea. A data set with more than 2000 thirty-minute averages, more than 1000 of which also contain wave information, has been used. The measurements were taken at a site in the middle of the Baltic Sea called Östergarnsholm. The measurements and the site are described in section 2. The wave influence of the marine atmospheric surface layer is discussed in section 3 as well as the turbulent kinetic energy budget. Section 4 describes the data used in the study and the different terms in the TKE-budget are presented in section 5. In section 6 results for the near-neutral range of this study are discussed in detail and in section 7 the consequences for the inertial dissipation method are outlined. A discussion of these findings with reference to previous studies is presented in section 8, and in section 9 the final conclusions are presented.

2. Site and Measurements

2.1. The Östergarnsholm Site

[15] Measurements were performed at Östergarnsholm, a small island (2 $\times$ 2 km) situated about 4 km east of the island of Gotland in the middle of the Baltic Sea (Figure 1). The Baltic is a semienclosed sea, almost surrounded by land areas. The Baltic Sea Proper (the part south of the Åland islands) extends from 54° to 60°N, and due to its high latitudes, the water temperature is quite low, and stable stratification is present for a large part of the year. Part of the Baltic Sea is also covered with ice during the winter.

[16] Östergarnsholm is a very flat island, with only sparse vegetation and no trees. On the southernmost tip, semicontinuous measurements have been performed on a 30-m tower, since May 1995.

[17] The base of the tower is situated at about 1 m above sea level, and the peninsula rises to no more than a couple of meters above sea level. There is an undisturbed over water fetch in the sector approximately 100–220°, and the distance to the shoreline in this direction is normally a few tens of meters.

[18] The slope of the seafloor outside Östergarnsholm is approximately 1:30 at 500 m from the shore. About 10 km from the peninsula, the depth is 50 m, reaching below 100 m further out. The slope of the seafloor outside Östergarnsholm permits an undisturbed wave field for most conditions [*Smedman et al.*, 1999]. However, during high wind speeds, a minor correction for limited water depth has to be applied. Thus, *Smedman et al.* [1999] found that for the measurements at the lowest turbulence measurement height (approximately 10 m) during neutral conditions, 90% of the flux originates from areas beyond 250 m, 50% originates from beyond 670 m and 70% from areas between 250 and

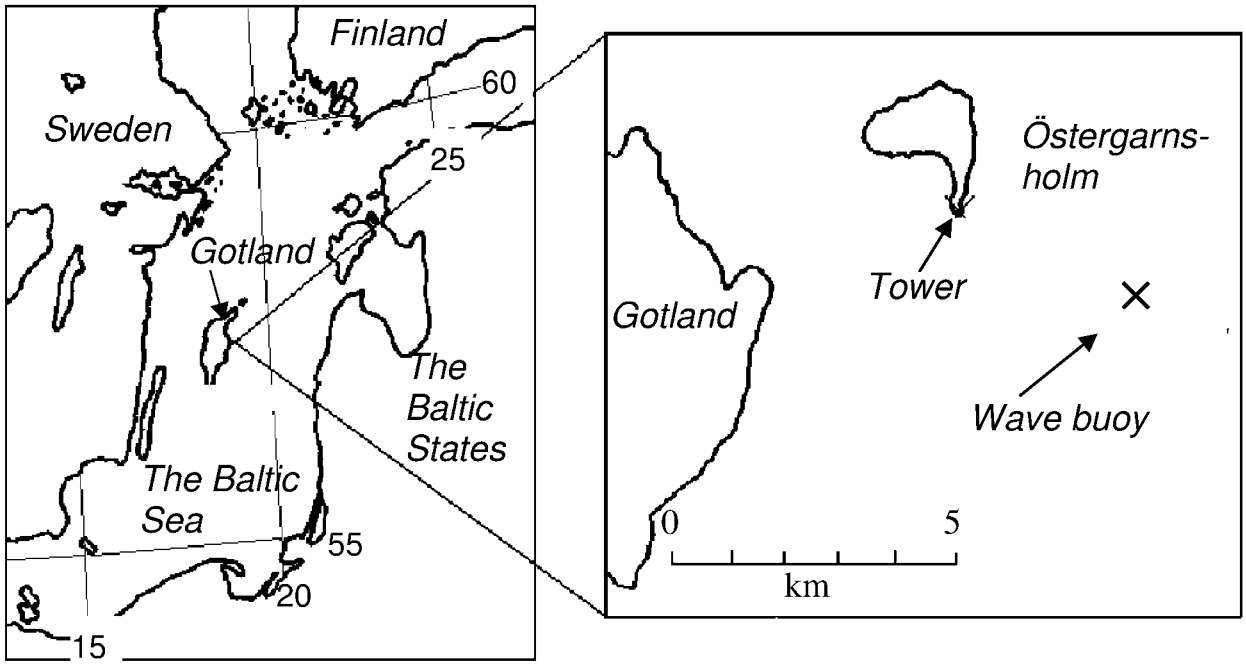

Figure 1. Map of the Baltic Sea, with a close-up on Östergarnsholm. The location of the wave buoy is also indicated.

1700 m. Thus it was concluded by *Smedman et al.* [1999, Appendix B] that "... even during the gale, the shallow water effects seem small at all elevations" (meaning the turbulent flux measuring heights, about 10, 18, and 26 m). Östergarnsholm will therefore represent open sea conditions of the Baltic Sea for most of the time when the wind is from the sector 100–220°.

[19] Since the Baltic Sea is semienclosed and limited in size, it can accommodate not more than one storm at a time. Most of the swell encountered at Östergarnsholm is produced in the southern part of the Baltic Sea and then propagated northward. This means that the swell observed at Östergarnsholm tends to be more unidirectional than is usually the case over the open ocean, where swell may result from several distant storms in different directions. It must therefore be kept in mind that the conditions concerning the effect of swell may be different in the open ocean. Thus there is a need for careful experiments in open ocean conditions to settle this question.

2.2. Tower Instrumentation

[20] Slow response ("profile") instruments are placed at five heights on the tower, at 7, 12, 14, 20, and 29 m above the tower base, measuring wind speed, wind direction, and temperature, with 1 Hz. Turbulence instruments (Solent Ultrasonic Anemometer 1012R2, Gill Instruments, Lymington, United Kingdom) are placed at 9, 17, and 25 m above the tower base and recorded with 20 Hz.

[21] The sonic anemometers were calibrated individually in a big wind tunnel before they were installed on the tower. The calibration procedure follows that of *Grelle and Lindroth* [1994], where the flow distortion made by the instrument itself is taken into account in a calibration matrix. From this, the three wind components are obtained. The lightweight cup anemometers placed at the five "profile" levels have also been individually calibrated in a big wind tunnel. They were recalibrated after many months of service in the field, with very reassuring results as concerns accuracy and stability of calibration.

[22] The temperature measured by the sonic anemometers T_s is very close (about 0.20%) to the virtual temperature, T_v (see appendix A). This is preferable since in calculating the Monin-Obukhov length, the virtual heat flux $\overline{w'\theta_v'}$ is used. The virtual heat flux has been corrected for "cross-wind" velocity contamination, since the signal is contaminated by the wind components normal to and along the path [*Kaimal and Gaynor*, 1991],

$$\overline{w'T_s'} \approx \overline{w'T_s'}(uncor) + 2U\frac{\overline{u'w'}}{R\gamma} \tag{1}$$

$\overline{w'T_s'}(uncor)$ is the uncorrected heat flux measured by the sonic, and R and γ are the universal gas constant and the specific heat ratio ($R\gamma$ = 403 m s^{-2} K^{-1}). U is the mean wind speed and $-\overline{u'w'}$ is the kinematic momentum flux. This correction seems to be most important in neutral and stable stratifications when the temperature fluctuations are small. In neutral conditions it can amount to a correction of about 20% [*Schotanus et al.*, 1983].

2.3. Wave Measurements

[23] In addition to the tower instruments, a Wave-Rider Buoy (owned and run by the Finnish Institute for Marine Research) is deployed about 4 km from Östergarnsholm (direction 115°, Figure 1), measuring sea surface (bucket) temperature, significant wave height, wave direction, and the spectra of the wave field. The buoy is moored at 36 m water depth. It is placed in the upwind fetch of the measurements, thereby representing the wave conditions in the "footprint area" outside Östergarnsholm. The wave meas-

urements have been performed semicontinuously during the same period as the tower measurements with the exception of wintertime periods with risk for ice damage.

[24] Wave data are recorded once an hour. The directional spectrum is calculated from 1600 s of data onboard the buoy. The spectrum has 64 frequency bands (0.025–0.58 Hz). The significant wave height is calculated by trapezoid method from frequency bands 0.05–0.58 Hz, and the peak frequency is determined by a parabolic fit [*Smedman et al.*, 1999].

2.4. Height Determination

[25] The actual height from the water level to the instruments on the tower varies due to varying sea level. Since all terms in the TKE-budget are normalized with the height to the instrument, it is important to use as good approximation of the height as possible, when different sea levels are to be compared. For example, using 10.0 m instead of 10.7 m (ref. below) would lead to a decrease in the values of the terms in the normalized TKE-budget with about 7%.

[26] Sea level measurements were made once an hour in Visby harbor on the west coast of Gotland. The measurements were performed by the Swedish Meteorological and Hydrological Institute (SMHI). Daily mean values of the measurements (H_{Visby}) have been recalculated to give an estimate of the sea level at Östergarnsholm. This is done by simply adding 3.2-H_{Visby} to the height of the instruments for each day. This correction (3.2 m) was obtained from measurements performed at Östergarnsholm in May 1995, where the height difference between the water level and the tower base was carefully measured. The difference was found to be 1.4 m for that particular case. For the data used, the height to the lowest turbulence instrument (9 m above tower base) will vary between 10.0 and 10.7 m, with an average of 10.4 m.

[27] It is not clear how rapidly the sea level east of Gotland (Östergarnsholm) responds to a sea level change on the west coast of Gotland (Visby), or vice versa, therefore only daily mean sea level measurements have been used.

3. Theoretical Considerations

3.1. Influence of Waves and Atmospheric Stability on the Marine Atmospheric Surface Layer

[28] The total stress at the sea surface $\tau = -\rho(\overline{iu'w'} + \overline{jv'w'})$ can be divided into three parts

$$\tau = \tau_{turb} + \tau_{wave} + \tau_{visc} \tag{2}$$

where τ_{turb} is the turbulent shear stress, τ_{wave} the wave induced stress and τ_{visc} the viscous stress; i and j are unit vectors in the longitudinal and lateral directions. For swell, that is waves traveling faster than the wind, τ_{wave} will be negative, and therefore reduce the total stress; values close to zero or even negative are not uncommon [e.g., *Volkov*, 1970; *Grachev and Fairall*, 2001; *Smedman et al.*, 1994]. During swell, pressure fluctuations will be induced by the waves and cause an upward transport of momentum. The influence of τ_{wave} will decrease with height, and the layer where τ_{wave} influences the measurements is usually called the wave boundary layer (WBL).

[29] To what height WBL reaches is currently under debate. *Drennan et al.* [1999b] discuss this, and show that in many studies the WBL is of the order 0.1 m. This was found for pure wind sea, but with swell the effects on turbulence statistics were evident at heights up to 12 m. Other studies have also showed that the WBL can extend up to considerable heights during swell [e.g., *Makova*, 1975; *Smedman et al.*, 1994; *Smedman et al.*, 1999].

[30] One way to describe how well developed the wave field is, is to use the so-called wave age, defined by

$$\text{Wave age} = c_0/(U_{10}\cos\theta) \tag{3}$$

where c_0 is the phase velocity of the waves at the peak of the spectrum, U_{10} the wind speed at 10 m, and θ the angle between wind and wave direction. Swell is here defined as $c_0/(U_{10}\cos\theta) > 1.2$ [cf. *Pierson and Moskowitz*, 1964]. The peak of the spectrum is defined as the highest peak in the wave spectrum, with no consideration taken to the number of peaks in the spectrum, i.e., if there are more than one peak and they are very close in magnitude, it is more or less random which one is taken as the highest value. Wave spectra with more than one peak is not uncommon in the Baltic Sea. Representing the waves by the wave age implies that most of the wave energy is contained in a narrow range around the peak frequency in the wave spectrum [*Grachev and Fairall*, 2001].

[31] Swell is usually related to low wind speeds, even if a swell component can be seen also at rather high wind speeds, in this study at as high as 12 m s^{-1}. *Grachev and Fairall* [2001] show for example that for wind speeds less than 2 m s^{-1} the momentum is transported purely from the ocean to the atmosphere.

[32] Swell is not an uncommon feature in the open oceans. *Drennan et al.* [1999a] found for example that for their 900 h of open ocean data, only 11% fell into the ideal category of stationary winds and pure wind sea. Much of the scatter seen in various data sets from measurements taken over the ocean is probably due to the fact that there is a swell component in the data that alters the characteristics [e.g., *Drennan et al.*, 1999a]. This is especially noticeable for data sets with low wind speeds. At the Östergarnholm site, swell occurs during 40% of the time [*Rutgersson et al.*, 2001].

[33] During pure wind sea conditions, *Drennan et al.* [1999b] find that the velocity spectra and cospectra follow the universal scaling law of *Miyake et al.* [1970], but in the presence of swell this is no longer satisfied. The normalized inertial subrange values during swell are for example higher than in pure wind sea. They also show that Monin-Obukhov scaling is not always justified in swell conditions, and that the standard transformation of meteorological data into neutral conditions is not valid.

[34] The stability and the wave age (equation 3) are closely connected. The stability parameter z/L is defined by

$$\frac{z}{L} = -\frac{zgk\overline{w'\theta_v'}}{u_*^3 T_0} \tag{4}$$

where L is the Monin-Obukov length and $\overline{w'\theta_v'}$ is the flux of virtual potential temperature. T_0 is a reference temperature in the surface layer, k is the von Karman constant, g the acceleration due to gravity, z the height of the measurements, and u_* the friction velocity defined as

$$u_*^2 = \left[\left(-\overline{u'w'}\right)^2 + \left(-\overline{v'w'}\right)^2\right]^{1/2} = \frac{|\tau|}{\rho} \tag{5}$$

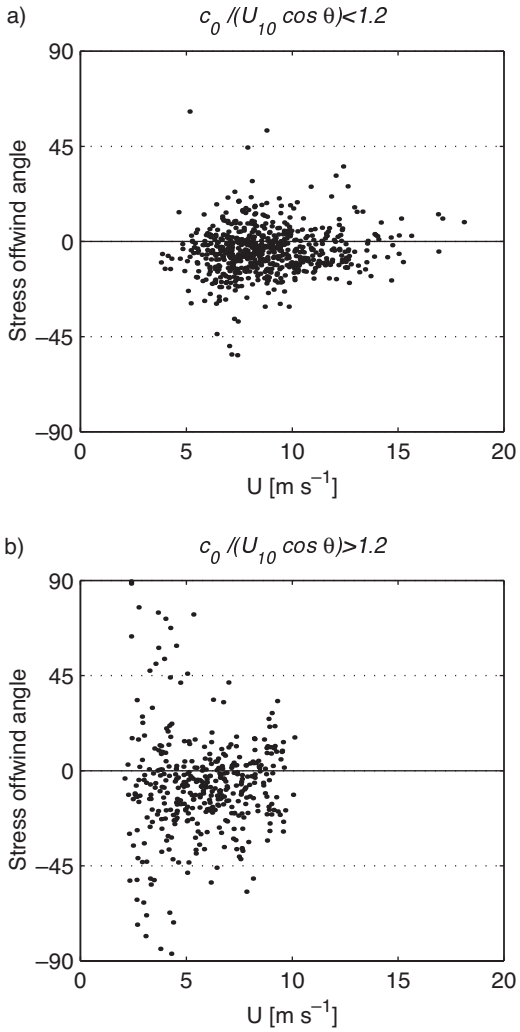

Figure 2. Relative angle of the stress vector to the mean wind direction, $\arctan(-\overline{v'w'}/-\overline{u'w'})$. (a) No swell data, $c_0/(U_{10}\cos\theta) < 1.2$, (b) swell data, $c_0/(U_{10}\cos\theta) > 1.2$.

Even if the heat flux can be large in some specific situations, it is usually of small magnitude and varies within a rather limited range. Then, variations in the magnitude of the friction velocity are likely to play a decisive role for the variation of z/L. As discussed above, during swell conditions, the total stress (τ) will be reduced or even negative and therefore u_* will become very small. Since u_* is in the denominator and raised to the third power, a small value can cause very large values of $|z/L|$, even if the heat flux is small.

[35] The friction velocity, u_* in equation (5) is determined from both $\overline{u'w'}$ and $\overline{v'w'}$. It is generally assumed that $\overline{v'w'}$ is small, and therefore gives negligible contribution to u_*. In swell conditions this is not always true. *Geernaert et al.*, [1993] showed that during light winds and near zero heat flux, the stress vector is not always aligned with the mean wind, but rather has a direction between the wind direction and the swell direction. That is, the direction of the swell plays an important role.

[36] In Figure 2, the relative angle of the stress vector to the mean wind direction, $\arctan(-\overline{v'w'}/-\overline{u'w'})$, is plotted against wind speed; Figure 2a shows the case with $c_0/(U_{10}\cos\theta) < 1.2$ and Figure 2b the case with $c_0/(U_{10}\cos\theta) > 1.2$. For low wind speeds and swell, the angle between the stress and the mean wind can be significant. This is in accordance with, for example, *Drennan et al.* [1999b]. For high wind speeds on the other hand, this difference is small.

[37] It has also been under discussion whether it is possible to use the inertial dissipation method during low wind speeds and swell conditions. This will be discussed in more detail in section 7.

3.2. The Turbulent Kinetic Energy Budget

[38] The TKE budget describes the physical processes that generate turbulence. It is given by

$$\underset{(S)}{\frac{\partial \bar{e}}{\partial t}} + \underset{(A)}{U\cdot\nabla\bar{e}} = \underset{(P)}{\overline{u'w'}\frac{\partial\bar{u}}{\partial z} + \overline{v'w'}\frac{\partial\bar{v}}{\partial z}} - \underset{(B)}{\frac{g}{T_0}\overline{w'\theta_v'}} + \underset{(T_t)}{\frac{\partial\overline{w'e'}}{\partial z}} + \underset{(T_p)}{\frac{1}{\rho}\frac{\partial\overline{p'w'}}{\partial z}} + \underset{(D)}{\varepsilon} \tag{6}$$

where $e' = 0.5(u'^2 + v'^2 + w'^2)$. ($S$) corresponds to local storage of TKE, (A) is advection of TKE by the mean wind, (P) corresponds to mechanical production of TKE from the mean flow, (B) buoyant production or loss, (T_t) turbulent transport, (T_p) pressure transport, and (D) molecular dissipation of TKE.

[39] *Stull* [1988] suggests that it is possible to neglect the storage term (S) and the advection term (A) over the ocean, since they are usually small. This is mainly due to the fact that the oceans do not experience a large diurnal cycle in the case of the storage term, and that advection is probably negligible even on small scales. The data has been subjectively checked for large variations over a small timescale, thereby removing data during frontal passages etc. Hence, assuming stationary and horizontally homogeneous conditions, equation (6) will be simplified to

$$\overline{u'w'}\frac{\partial\bar{u}}{\partial z} + \overline{v'w'}\frac{\partial\bar{v}}{\partial z} - \frac{g}{T_0}\overline{w'\theta_v'} + \frac{\partial\overline{w'e'}}{\partial z} + \frac{1}{\rho}\frac{\partial\overline{p'w'}}{\partial z} + \varepsilon = 0 \tag{7}$$

Normalizing equation (7) with kz/u_*^3 gives

$$\frac{kz}{u_*^3}\left(\overline{u'w'}\frac{\partial\bar{u}}{\partial z} + \overline{v'w'}\frac{\partial\bar{v}}{\partial z}\right) - \frac{kz}{u_*^3}\frac{g}{T_0}\overline{w'\theta_v'} + \frac{kz}{u_*^3}\frac{\partial\overline{w'e'}}{\partial z} + \frac{kz}{u_*^3}\frac{1}{\rho}\frac{\partial\overline{p'w'}}{\partial z} + \frac{kz}{u_*^3}\varepsilon = 0 \tag{8}$$

which is the same as

$$\underset{(PN)}{\phi_m} - \frac{z}{L} - \underset{(BN)}{\phi_t} - \underset{(T_tN)}{\phi_p} = \underset{(T_pN)\ (DN)}{\phi_\varepsilon} \tag{9}$$

[40] The two transport terms (T_tN) and (T_pN) are often assumed to be negligible or equal in magnitude (with opposite sign), at least in near neutral conditions. However, there have not been so many studies where these terms have actually been measured. All the terms in the budget will be discussed in more detail in section 5.

4. Data

[41] Measurements from the period May 1995 to December 1997 have been used. Only measurements with long

(more than 150 km) over water fetch have been analyzed, leaving 2166 thirty-minute averages at the lowest height of measurements, where 1033 also contain wave information. Thirty-minute averages have been used for both the turbulence and profile measurements. The wave data are measured once an hour. Only measurements at the lowest sonic anemometer level (about 10 m) are presented here. Data from the other heights will be analyzed in a forthcoming paper.

[42] Climatological statistics are shown in Figure 3. Figure 3a shows the wind speed distribution and Figure 3b the frequency distribution of the stability parameter z/L (equation 4). Data with wind speed less than 2 m s^{-1} has been removed due to instrument uncertainties. The most common wind speed is between 6 and 10 m s^{-1}, and most of the data are in neutral or near neutral conditions (there are also a few data points outside this plot). The wave age, $c_0/(U_{10}\cos\theta)$ (equation 3), distribution is shown in Figure 3c. Most of the data has a wave age around one. Notice that the amount of data is not the same as in Figures 3a and 3c, because wave data were not available for all the tower data, and values with negative wave age and more than 90° angle between wind and wave directions have been removed.

5. Terms in the Turbulent Kinetic Energy Budget

[43] The terms in the TKE-budget are here defined so that a positive value indicates a gain in energy and a negative value a loss.

5.1. Mechanical Production

[44] The normalized mechanical production (PN), which is the same as the normalized wind gradient, ϕ_m is defined as

$$PN = \phi_m - \frac{kz}{u_*^3}\left(\overline{u'w'}\frac{\partial U}{\partial z} + \overline{v'w'}\frac{\partial V}{\partial z}\right) \tag{10}$$

where U and V are the mean wind speeds in along- and crosswind direction.

[45] It has been under discussion whether the ϕ_m-functions determined over land also are valid over sea, and if the Monin-Obukhov similarity theory can be applied in the marine atmospheric boundary layer. Over land, many experiments have been made to determine the ϕ_m-functions [*Wyngaard and Cote*, 1971; *Businger et al.*, 1971; *Högström*, 1987], but over sea the data are fewer.

[46] To be able to calculate both $\partial U/\partial z$ and $\partial V/\partial z$, gradients from the three sonic anemometers have to be used. Unfortunately, these gradients turned out to be very uncertain compared to the gradients from the profile measurements. But, the influence of the term $-\overline{v'w'}(\partial V/\partial z)$ was small compared to $-\overline{u'w'}(\partial U/\partial z)$ when using the gradients from the sonic anemometers. However, $\overline{v'w'}$ can not be neglected in calculating u_*, especially during swell (see section 3). Equation 10 can therefore be simplified to

$$PN = \phi_m = -\overline{u'w'}\frac{kz}{u_*^3}\frac{\partial U}{\partial z} \tag{11}$$

[47] The wind gradient, $(\partial U/\partial z)$, was therefore derived by a second-order polynomial from a best fit to the log-lin plot of wind speed measurements from the five cup anemometers on the tower. For most of the data all five anemometers were working, but for some periods only three or four are used. The gradient has been calculated at the height of the turbulence measurement (about 10 m) from the fitted curve. The second-order polynomial fit was chosen

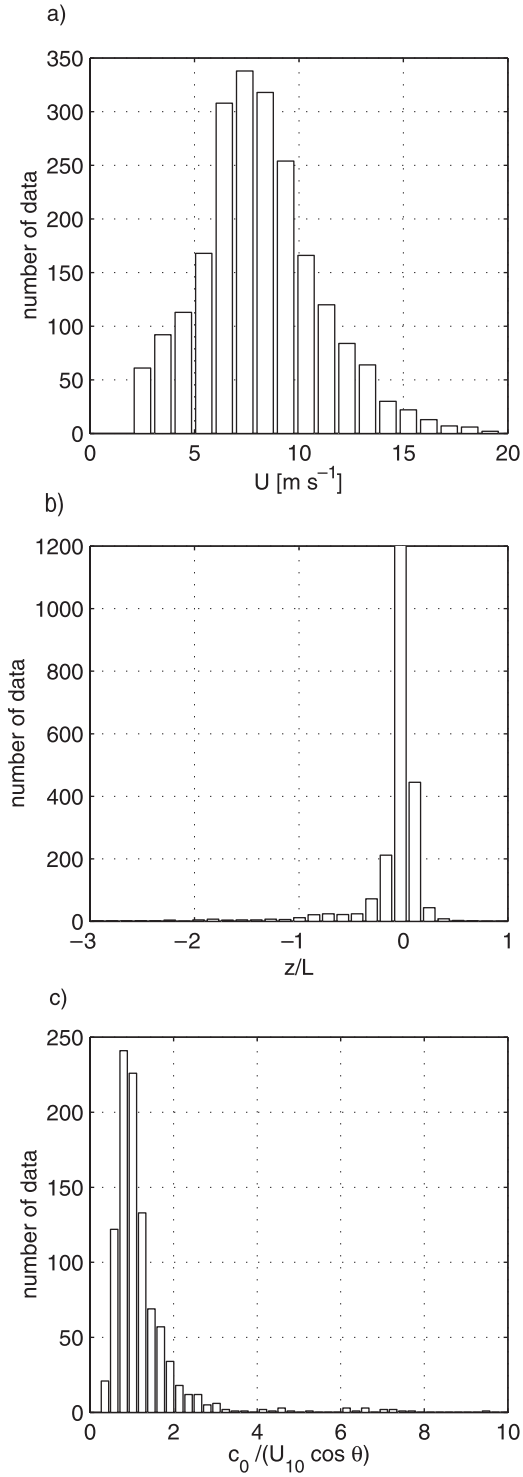

Figure 3. Climatological statistics for the data used. (a) Wind speed distribution at approximately 10 m, where only data above 2 ms^{-1} has been included, (b) stability distribution, a few points are outside the plot (c) wave age distribution, only positive values with (wave direction − wind direction) <90° showed.

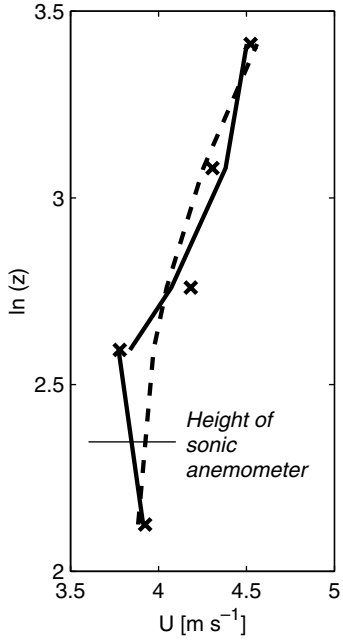

Figure 4. Example of a wind profile during swell ($c_0/(U_{10}$ cos θ) = 2.5), with a so-called "wave-driven wind," 25 August 1996, 1730. Crosses (×) are the five anemometers, hatch line: a second-order polynomial fitted to all five anemometers. The lowest part of the solid line is fitted to the two lowest anemometers, while the higher is fitted to the four uppermost anemometers.

instead of a finite differencing, since even though the profile measurements are much better than those from the sonic anemometers, the finite differencing method would be very sensitive to the absolute value of each sensor. The result is, however, the same on average, but the spread becomes much larger with finite differencing.

[48] But, there can be some problems with fitting an "acceptable" curve to the wind speed measurements. It is not uncommon that the lowest wind speed measurement is influenced by the waves, especially in swell conditions, giving rise to a so-called wave-driven wind [*Smedman et al.*, 1999]. Figure 4 shows an example of this type of wind gradient.

[49] If only the two lowest anemometers (lowest part of the solid line) are used to determine the wind gradient at the height of the sonic anemometer, the gradient might be negative, giving a negative value of ϕ_m. On the other hand, when a second-order polynomial is fitted to all five anemometers (dashed line), the gradient at the height of the sonic anemometer might be different from the one determined with only the two lowest anemometers.

[50] All the fitted curves have been manually checked and compared to the actual wind speed measurements, and if the deviation between them was too large (more than approximately 1%) that measurement was rejected to avoid this problem.

5.1.1. The von Karman Constant

[51] The value of the von Karman constant (k) is crucial in calculating ϕ_m (equation 11). One of the most controversial questions in boundary layer meteorology is the value of this constant. Values from 0.35 to 0.65 can be found in the literature, but it seems that the value 0.40 is the most common. Results from the Kansas experiment [e.g., *Businger et al.*, 1971] suggested k = 0.35. *Tennekes* [1973] concludes that k is a function of the surface Rossby number and therefore suggests 0.35 for smooth terrain and 0.40 for rough terrain.

[52] *Högström* [1985, 1996] analyzes several atmospheric data sets from various types of surfaces (including the ocean) and finds no dependence with either the Rossby surface number or the roughness, and concludes that $k = 0.40 \pm 0.01$. He also suggests that much of the variation reported in earlier measurements are due to measurement errors, such as flow distortion. In agreement with the recommendation of *Högström* [1996], k = 0.40 has been used in this study.

5.1.2. Mechanical Production as a Function of Stability

[53] The calculated ϕ_m values are shown in Figure 5 as a function of stability. Figure 5a shows all the data (dots), the bin averaged values with error bars (solid line), and the (m curve suggested by *Högström* [1996] (dashed line). For unstable data ($-z/L > 0.5$), almost all ϕ_m values are very small or negative. This is due to influence of swell (see discussion in section 3). Looking at the more near neutral

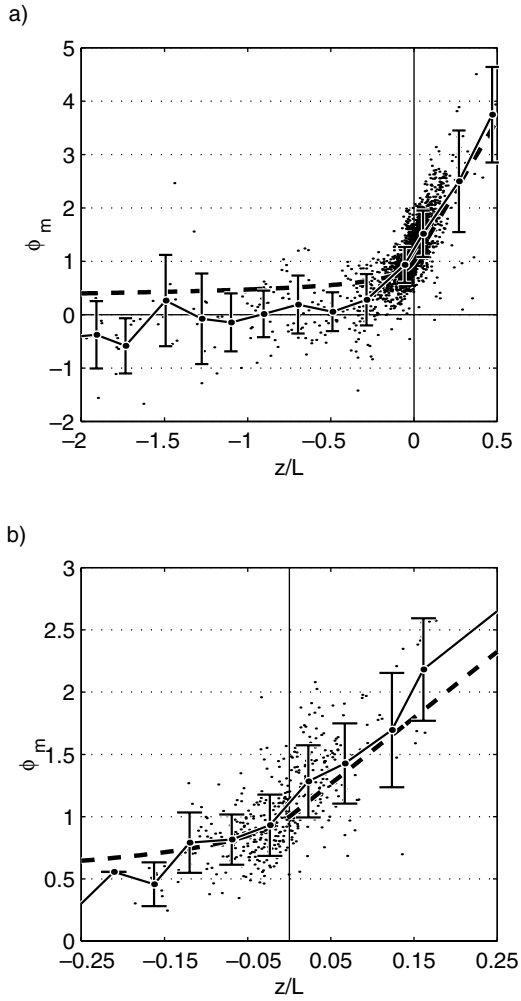

Figure 5. Normalized mechanical production, ϕ_m as a function of stability, dots (●) are all the measurements, the solid line is bin-averaged mean values, and dashed line the curve of *Högström* [1996]. (a) All values, (b) values with wave age $0.5 < c_0/(U_{10}$ cos θ) < 1.

data, the curve falls off much more rapidly when moving toward convective conditions than the curve suggested by *Högström* [1996]. One explanation for this is that swell also influences at higher wind speeds and neutral conditions.

[54] This can be compared to Figure 5b where only measurements in the wave age range $0.5 < c_0/(U_{10} \cos \theta) < 1$ have been used in an attempt to avoid the wave influence (both very young and old waves have been excluded). Most low and the negative ϕ_m-values have now disappeared, but the measured curve is still slightly beneath Högström's during unstable conditions ($z/L < -0.15$). For stable conditions, the averaged curve is approximately the same as Högström's, or perhaps slightly higher.

5.2. Buoyancy

[55] The normalized buoyancy production or loss (BN) is the same as the stability parameter ($-z/L$) (equation 4). For unstable stratification this will be a gain of turbulent kinetic energy (production), and for stable stratification a loss (destruction). For neutral conditions this terms will obviously be equal to zero. As discussed in section 3, the variation in normalized buoyancy is more related to the variation of u_* rather than of the heat flux itself.

5.3. Dissipation

[56] The normalized dissipation (DN) is defined as

$$DN = -\phi_\varepsilon = -\frac{\varepsilon kz}{u_*^3} \tag{12}$$

and will always exist when TKE is nonzero. The dissipation was determined from spectral measurements within the inertial subrange assuming Kolmogorov similarity:

$$\kappa S(\kappa) = \alpha \varepsilon^{2/3} \kappa^{-2/3} \tag{13}$$

where α is the Kolmogorov constant, and κ the wave number. Applying Taylor's hypothesis:

$$\kappa = \frac{2\pi n}{u_{apparent}} \tag{14}$$

n is the frequency, and only the apparent wind speed $u_{apparent}$ (which is equal to the wind speed in fix point measurements but the relative wind speed in the case of measurements from a moving ship or aircraft) is needed. This gives:

$$\varepsilon = \left[\frac{nS_u(n)}{\alpha}\right]^{3/2} \cdot n \cdot \frac{2\pi}{u_{apparent}} \tag{15}$$

and from this the normalized dissipation, $\phi_\varepsilon = \left(\varepsilon kz/u_*^3\right)$ can be determined.

[57] The dissipation was determined from manually checked spectra of longitudinal wind velocity. If the slope of the inertial subrange was approximately $-2/3$, a log-log fit of the values in the inertial subrange was performed, and values of $nS_u(n)$ and frequency n, was calculated from this curve. Spectra that did not fulfil the above requirements have been rejected.

5.3.1. Kolmogorov's Constant

[58] The magnitude of the normalized dissipation is very sensitive to the choice of Kolmogorov's constant α. From a review of values quoted in the literature, *Högström* [1990] concludes that $\alpha = 0.52 \pm 0.02$. All values used in that study were based on simultaneous direct measurements of dissipation and inertial subrange spectra. Values within this range seem to be the mostly used [e.g., *Schacher et al.*, 1981; *Fairall and Larsen*, 1986; *Smith et al.*, 1992]. A value of 0.55 is also commonly suggested [*Large and Pond*, 1981, 1982; *Anderson*, 1993; *Donelan et al.*, 1997]. *Fairall and Larsen* [1986] estimate the uncertainty in the Kolmogorov constant to be approximately 20%.

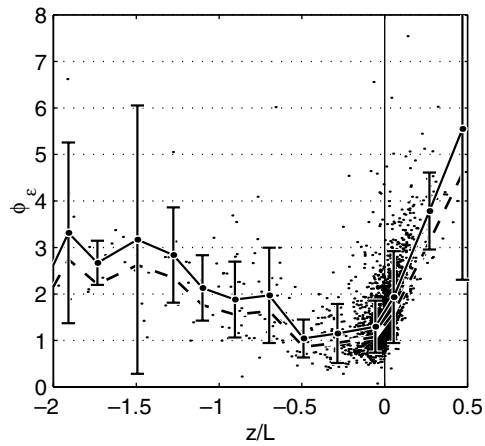

Figure 6. Minus the normalized dissipation as a function of stability, see Figure 5 for explanations of the symbols. Dashed line (−−) is the average curve with $\alpha = 0.59$.

[59] One way to account for a possible imbalance between production and dissipation is to use an "apparent" Kolmogorov constant (α_a), which will only be equal to the true Kolmogorov constant if the assumption of balance between production and dissipation holds true. *Deacon* [1988] gives an average value of 0.62 for neutral to moderately unstable conditions, but suggests that 0.59 ± 0.025 should be used over sea. *Högström* [1996] comes up with 0.59, while *Yelland and Taylor* [1996] suggest a lower value, 0.55. *Fairall et al.* [1990] show that changing the Kolmogorov constant from 0.52 to 0.59 would represent a decrease of roughly 13% in the stress estimates. In agreement with the recommendation of *Högström* [1996], the value 0.52 has been used here.

5.3.2. Dissipation as a Function of Stability

[60] Minus the normalized dissipation ($-DN$) is presented in Figure 6 as a function of stability. Notice that the sign is changed to positive (i.e., dissipation is by definition a loss in energy). Dissipation has a broad minimum somewhere in the range $-0.50 < z/L < 0$, which is in accordance with other studies, both from measurements over land [e.g., *Högström*, 1990] and over sea [e.g., *Schacher et al.*, 1981]. Also shown (dashed line) is the average curve when 0.59 is used as an apparent Kolmogorov constant, α_a.

5.4. Transport Terms

[61] The transport terms in the TKE-budget (equation 9) are often neglected [*Wyngaard and Cote*, 1971; *Hicks and Dyer*, 1972; *Large and Pond*, 1981; *Fairall and Larsen*, 1986; *Edson et al.*, 1991; *Smith et al.*, 1992], and a balance between local production and dissipation is assumed, at least in near-neutral conditions. There is a considerable

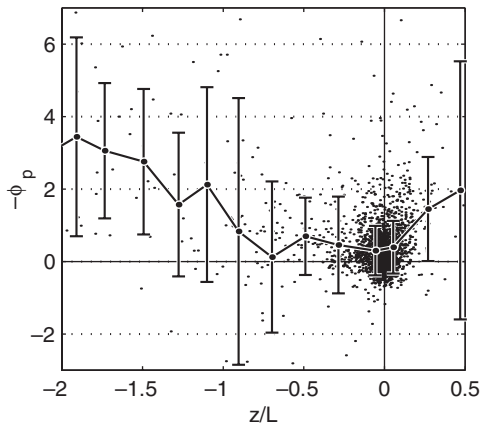

Figure 7. Normalized pressure transport as a function of stability, see Figure 5 for explanations of the symbols.

controversy about the validity of these assumptions, and it is obvious that this needs to be further evaluated.

[62] Some attempts have been made to parameterize the sum of the transport terms, *Dupuis et al.* [1995, 1997] suggest that it depends on stability for unstable stratification. *Yelland and Taylor* [1996] on the other hand, claim that the sign and magnitude is a function of both stability and wind speed.

5.4.1. Turbulent Transport

[63] The normalized turbulent transport (T_tN) is defined as

$$T_tN = -\phi_t = -\frac{kz}{u_*^3}\frac{\partial \overline{w'e'}}{\partial z} \tag{16}$$

[64] It represents the divergence of the turbulent flux of kinetic energy. This term does not produce, nor destroy TKE, it just moves it, and when integrating over the whole boundary layer the sum will be zero.

[65] The turbulent transport was determined from measurements of $\overline{w'e'}$ at the lowest level (about 10 m) and the middle level (about 18 m). This means more precisely that the turbulent transport presented for the lowest level is actually taken at a height of approximately 14 m. The turbulent transport was found to be small during all stability conditions although the scatter is large. This will be discussed more in section 6.

5.4.2. Pressure Transport

[66] The normalized pressure transport (T_pN) is defined as

$$T_pN = -\phi_p = -\frac{kz}{u_*^3}\frac{1}{\rho}\frac{\partial \overline{p'w'}}{\partial z} \tag{17}$$

[67] It represents the transfer of energy from one level to another due to pressure fluctuations. This term is very difficult to measure directly, because pressure fluctuations are very small (on the order of 0.05 hPa) compared to large scale fluctuations, and the measurements of the pressure transport term are often contaminated by the large scale variations. There are, however, some studies where the pressure transport has been measured directly [e.g., *Wilczak et al.*, 1999].

[68] T_pN is the only term in the TKE-budget that was not determined directly in this study. Instead, it was calculated as a residual from the other terms. One should keep in mind that errors in calculating the other terms will add up in this term. Also possible errors from assuming stationary and homogeneous conditions will contribute to uncertainties in T_pN.

5.4.2.1. Pressure Transport as a Function of Stability

[69] Contrary to the normalized turbulent transport, the normalized pressure transport is not negligible even in neutral conditions (Figure 7). This is in accordance with other studies and will be discussed more in the next section.

5.5. Imbalance

[70] The normalized imbalance is defined as the difference between normalized production and normalized dissipation, which by definition is the same as the sum of the transport terms. But as discussed above, T_tN is small during the conditions encountered here, so the main contribution to the imbalance will come from T_pN.

[71] *Wyngaard and Coté* [1971] find, from measurements over land, that during stable conditions dissipation equals shear production, but during unstable conditions dissipation slightly exceeds production, and the turbulent transport becomes significant in transporting energy upwards. *Edson and Fairall* [1998], on the other hand, find a balance between production and dissipation over sea, except for slightly unstable conditions where production exceeds dissipation. A possible explanation for this might be that over developing waves, part of the energy flux generates waves and currents, rather than being dissipated into thermal energy. *Wilczak et al.* [1999] also find from measurements over the ocean that production exceeds dissipation for slightly unstable conditions, otherwise dissipation exceeds production.

5.5.1. Imbalance as a Function of Stability

[72] The normalized imbalance is plotted in Figure 8 against stability. The bin-averaged values indicate that the dissipation is larger than production during all stabilities, also at neutral conditions, though the smallest values of the imbalance is found at neutral stability. The imbalance increases as we move away from neutral conditions, but increases much more quickly on the stable side than on the unstable side. Also shown (dashed line) is the average curve resulting from using α_a = 0.59 (as in Figure 6). The

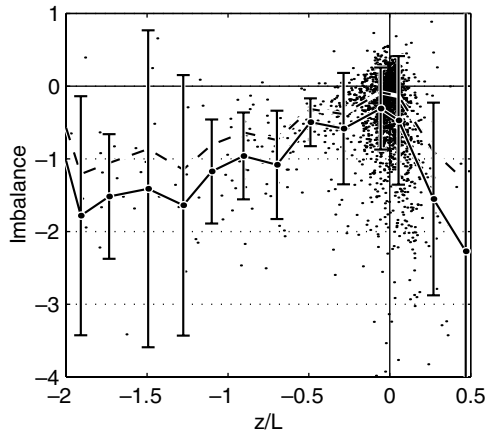

Figure 8. Normalized imbalance (normalized production-normalized dissipation) as a function of stability, see Figure 5 for explanations of the symbols. Dashed line (−−) is the average curve with α = 0.59.

imbalance then becomes smaller, especially for neutral conditions.

[73] However, there is significant scatter in the individual data points, especially in the near neutral data, where both positive and negative values can be found. This might indicate that the imbalance does not only depend on stability, but also on some other physical parameters. Using an apparent Kolmogorov constant of 0.59 will decrease the imbalance on average, but the scatter is the same, with both positive and negative values. In the next section, the near neutral data will be investigated in more detail, and it will be shown that the imbalance also depends strongly on wave age and wind speed. Therefore, using $\alpha_a = 0.59$ will only make the imbalance zero for some conditions.

6. Results for Near-Neutral Conditions

[74] As shown above, the terms in the TKE-budget have a clear stability dependence, and there is a large difference between the stable and unstable side (Figures 5–8). But, it is of course possible that the waves will influence the measurements as well. The scatter of the individual data points might be an indication of this.

[75] The wave age, $c_0/(U_{10}\cos\theta)$, was defined in section 3 as a parameter to describe the wave influence. The wave state can be divided into three different types according to wave age. Small wave ages, $c_0/(U_{10}\cos\theta) < 0.50$, where waves are growing; high wave ages, $c_0/(U_{10}\cos\theta) > 1.2$, is defined as swell, where the waves are traveling faster than the wind, and the waves are in a decaying state. Between these two wave states, i.e., $0.5 < c_0/(U_{10}\cos\theta) < 1.2$, the waves are in a saturated condition, neither growing, nor decaying. As will be shown in this section, the sea surface then acts as a land surface on the atmospheric flow.

[76] In section 3 it was discussed that the total stress (i.e., sum of turbulent shear stress, wave induced stress and viscous stress), will be reduced or even negative during swell conditions (equation 2), since the wave induced part will be in opposite direction to the turbulent stress. This will then lead to a decreased value of u_* (equation 5). The small value of u_* during swell will also affect the stability parameter z/L (equation 4), since it will give a large value of $|z/L|$, even if the heat flux is small. This means that z/L does not only act as a stability parameter, but is also influenced by the waves. For some swell situations, this influence can be seen up to considerable heights [e.g., *Smedman et al.*, 1994].

[77] To be able to distinguish between the stability dependence and the wave influence, only near neutral data will be considered in this section, and the terms in the TKE-budget will be plotted as a function of two variables, stability (z/L) and wave age ($c_0/(U_{10}\cos\theta)$) or stability (z/L) and wind speed (U). The data has been bin-averaged in two dimensions, and the numbers inside the plot are the averaged values of the specific term. As earlier, positive values indicate a gain in energy and negative values a loss. The dashed lines in the figures are drawn subjectively.

[78] In Figure 9a, the normalized mechanical production (PN) is plotted as a function of wave age and stability. PN is approximately 1.0 at neutral conditions, but the values increase rapidly on the stable side ($z/L > 0$). PN decreases for increasing instability, and also to some degree with increasing wave age. Otherwise the influence of the wave age seems to be quite small.

[79] In Figure 9b PN is given as a function of stability (z/L) and mean wind speed (U). There is of course a strong correlation between wind speed and wave state, high wind speed (>8 m s^{-1}) being likely to be associated primarily with wind waves and low wind speed (<6 m s^{-1}) with swell. The decrease in PN with z/L is more pronounced for low wind speeds, again indicating the influence of swell. The stability dependence seen in both figures could also be seen in Figure 5, where the slope of the curve in the near-neutral range is quite steep.

[80] Figure 10 shows minus the normalized dissipation ($-DN$) as a function of stability and wave age. Notice that the sign is changed to positive (i.e., dissipation is by definition a loss in energy). $-DN$ increases with increasing wave age for neutral conditions, but the minimum of $-DN$ is for swell and unstable conditions. During stable conditions, $-DN$ increases when stability and wave age increase, even if there is a maximum for $-DN$ also at small wave ages.

[81] The two transport terms are shown in Figure 11. The normalized turbulent transport (T_tN) in Figure 11a has some scatter, but is clear that the values are small or very close to zero for all stabilities and wave ages. T_tN does not balance the normalized pressure transport (T_pN), which is shown in Figure 11b. The pressure transport has a clear dependency on both stability and wave age. For small wave ages the pressure transport is negative, it changes sign at $c_0/(U_{10}\cos\theta) \approx 0.50$. Between $c_0/(U_{10}\cos\theta) \approx 0.50$ and 1.2 the value is approximately 0.25, and for swell $c_0/(U_{10}\cos\theta) > 1.2$, T_pN becomes significant.

[82] $T_pN \approx 0.25$ is in accordance with *Högström* [1996], who refers to an experiment over land at Laban's Mills in Sweden, where (T_pN) was found to be 0.25 and (T_tN) zero. This is explained by *Högström et al.* [2002] as a result of surface-layer-scale structures playing a decisive role in the momentum transport in the neutral atmospheric surface layer.

[83] Most of the imbalance, normalized production-normalized dissipation (Figure 12a), therefore originates from the pressure transport. The values are almost the same as the values for T_pN, but the sign is the opposite. For small wave ages, $c_0/(U_{10}\cos\theta) < 0.50$, production exceeds dissipation, energy is building up the waves rather than being dissipated into heat. For moderate wave ages $0.50 < c_0/(U_{10}\cos\theta) < 1.2$, the imbalance resembles that found over land [e.g., *Högström*, 1996]. For swell $c_0/(U_{10}\cos\theta) > 1.2$, dissipation is much larger than production.

[84] The same structure is also found in Figure 12b, where the imbalance is plotted as function of stability and wind speed. At high wind speeds production exceeds dissipation, and at low wind speeds the dissipation is much larger than the production. The same stability dependence as in Figure 8 can also be seen in Figures 12a and 12b, with larger imbalance as we move away from neutral conditions.

[85] The results in this section have some important implications for the inertial dissipation method. This will be discussed in the next section.

7. The Inertial Dissipation Method

[86] As described earlier, the inertial dissipation method builds on estimating u_* from the TKE-budget. The terms in

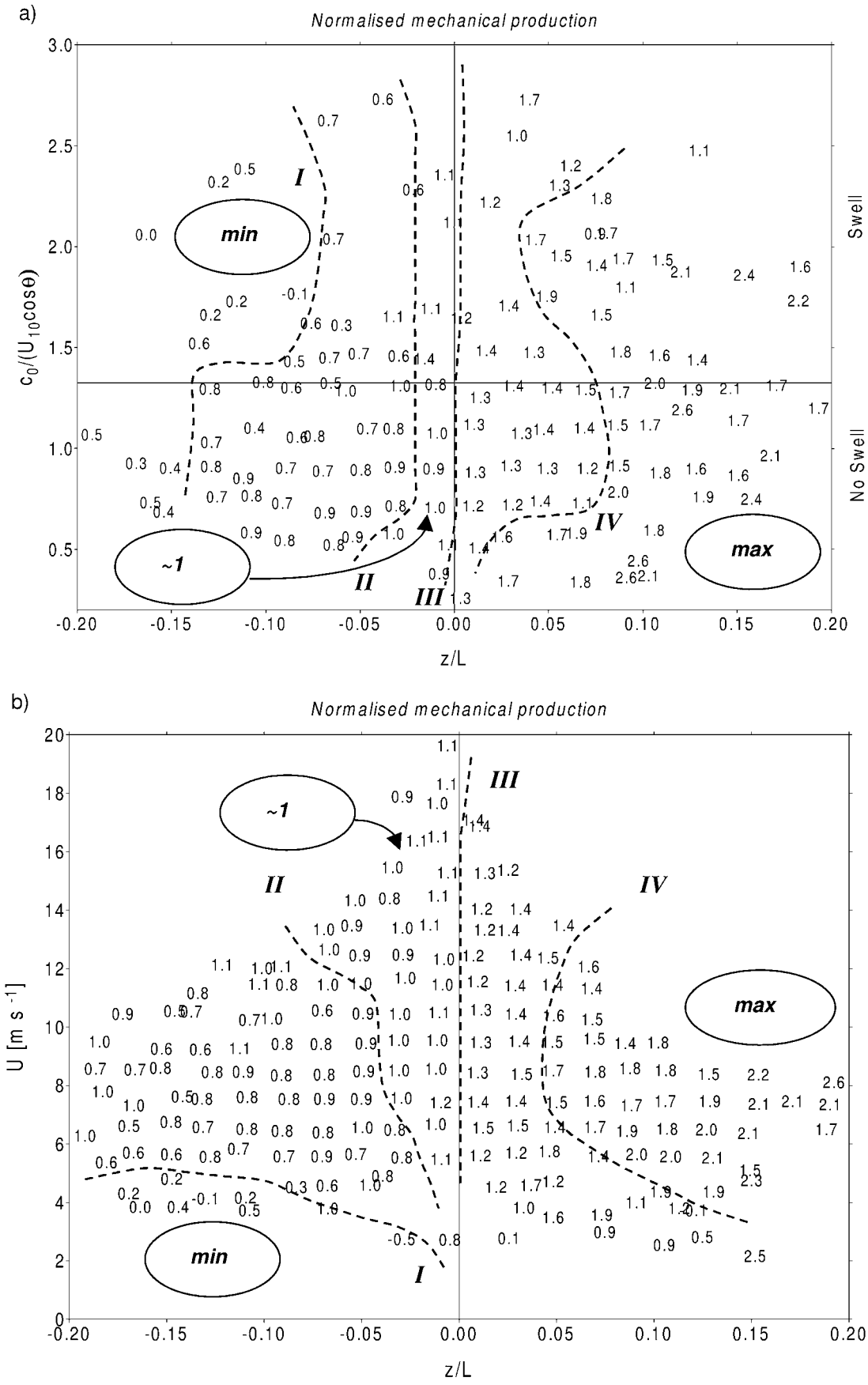

Figure 9. Normalized mechanical production as a function of stability and (a) wave age, (b) wind speed. Curves: (*I*) $PN \sim 0.5$, (*II*) $PN < 1$, (*III*) $PN > 1$ and (*IV*) $PN \sim 1.5$.

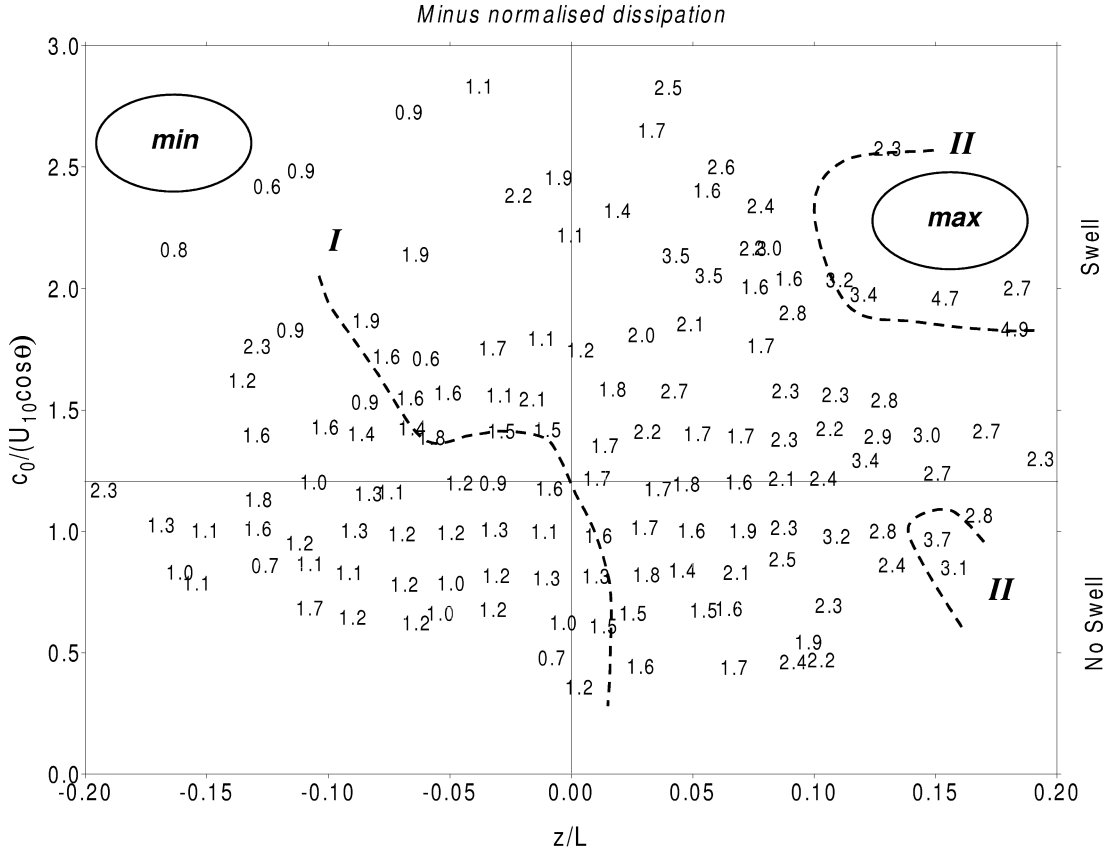

Figure 10. Minus the normalized dissipation ($-DN$) as a function of stability and wave age. Curves: (*I*) $DN \sim 1.5$ and (*II*) $DN \sim 3$.

the budget must then be known. Solving for u_* in equations 9, 12 and 15 gives:

$$u_* = \left[\frac{nS_u(n)}{\alpha}\right]^{1/2}\left[\frac{2\pi}{u_{apparent}}\cdot\frac{kz}{\phi_m - z/L - \phi_t - \phi_p}\cdot n\right]^{1/3} \quad (18)$$

It is then possible to calculate the momentum flux τ

$$\tau = \rho u_*^2 \quad (19)$$

This usually involves an iterative process, since L is needed to calculate u_*, and u_* is needed to calculate L (see equation 4). Problems with convergence in not uncommon by using this method. It is also a problem how to estimate the flux of virtual potential temperature $w'\theta_v'$ (equation 4). *Dupuis et al.* [1997] suggested two methods, either to use of a bulk formula or to use dissipation rates for the temperature in each step. The last method can, however, be troublesome if a clear inertial subrange in the temperature spectra can not be found from the measurements, which is quite common due to instrumental problems.

[87] It should also be remembered that the inertial dissipation method only gives positive values of the flux, so some indicator for swell cases when the momentum transport is upward is also needed.

[88] The use of the traditional inertial dissipation method (assuming that the transport terms are small) has been questioned by some authors, and especially for cases with swell [*Donelan et al.*, 1997; *Drennan et al.*, 1999b]. *Drennan et al.* [1999b] how that flux measurements with the eddy-correlation method were approximately twice the calculated fluxes with the inertial dissipation method when strong swell was present. In pure wind sea, the agreement with the eddy-correlation method was excellent [*Donelan et al.*, 1997].

[89] An interesting fact is also that a wave influence is difficult to see in measurements with the inertial dissipation method. *Drennan et al.* [1999a] compared measurements of the drag coefficient made with the inertial dissipation method and the eddy-correlation method. It is clear that the measurements made with the eddy-correlation method showed a sea state dependence, while the inertial dissipation method did not. *Yelland and Taylor* [1996] claim that their measurements made with the inertial dissipation method show hardly any sea state dependence.

[90] The difference between the eddy-correlation method and the inertial dissipation method might also be seen for high wind speeds and low wave ages. *Janssen* [1999] discusses the lack of scatter in the drag coefficient obtained with the inertial dissipation method and found no wave influence, which is then in contrast to measurements performed with the eddy-correlation method. His explanation is that the pressure transport is not included in the inertial dissipation method. By using a wave model, he shows that pressure transport is important in the presence of wind generated ocean waves and high wind speeds (>15m s^{-1}), and that this might increase the surface stress with about

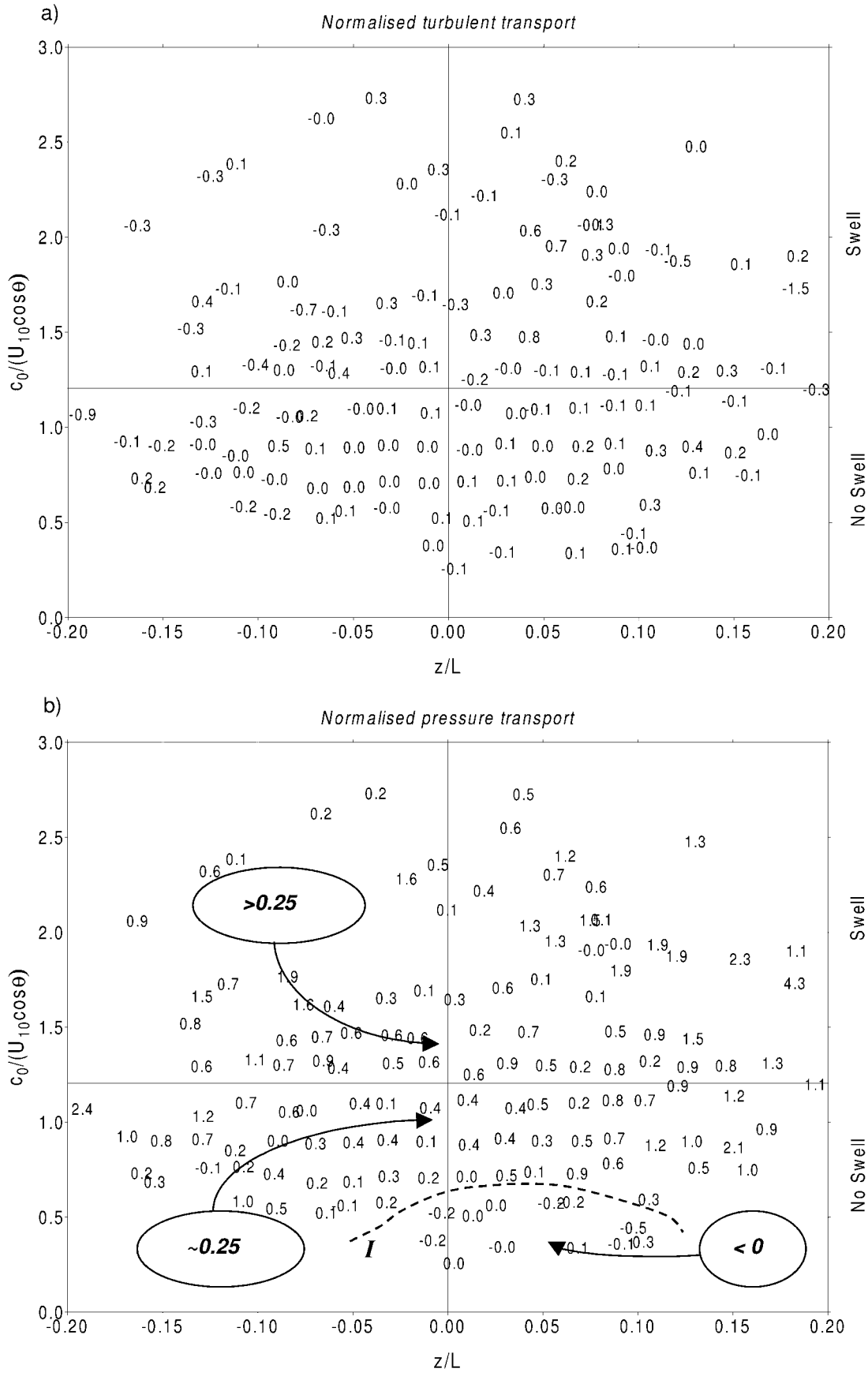

Figure 11. Normalized transport terms as a function of stability and wave age. (a) Normalized turbulent transport, (b) normalized pressure transport. Curve: (*I*) $T_pN \sim 0$.

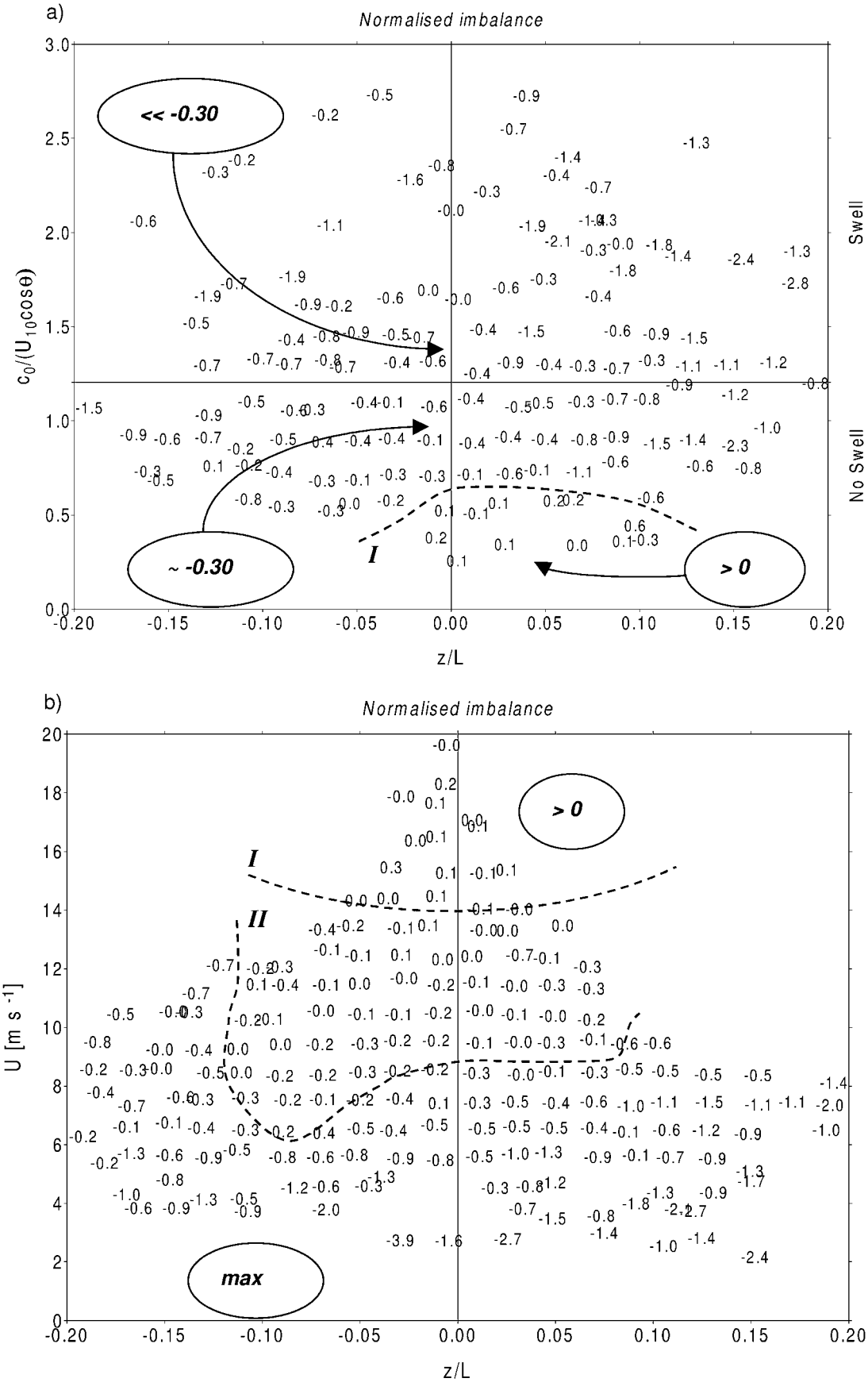

Figure 12. Normalized imbalance (normalized production-normalized dissipation) as a function of stability and (a) wave age, (b) wind speed. Curve: (*I*) *Imbalance* ~ 0 and (*II*) *Imbalance* ~ -0.25.

20%. *Taylor and Yelland* [2001] do not agree with *Janssen* [1999]. They claim that they see no wave age dependency in their data.

[91] An explanation for these seemingly contrasting results may be that the inertial subrange does not react in the same way as the whole spectrum. The influence of swell is contained in frequencies between 0.06 and 0.16 Hz [*Rieder and Smith*, 1998], and the inertial subrange is usually located at higher frequencies. This is in accordance with *Drennan et al.* [1999b], who show that the inertial subrange during swell follow the pure wind sea data well, while the lower frequencies do not.

[92] A. Smedman, U. Högstrom, and A. Sjöblom (A note on velocity spectra in marine boundary layer, submitted to *Boundary-Layer Meteorology*, 2002) also show that for some swell situations the inertial subrange is not affected by swell. During decreasing wind conditions (increasing wave ages), the frequency range where the wave influence can been seen is increasing toward higher frequencies. However, it will take some time before all of the inertial subrange will be affected. Hence, if we measure in the high-frequency part of the inertial subrange, it may not be certain that the swell influence has reached at that frequency yet. Therefore the measurements do not show the same wave influence that would be seen if the whole spectrum was affected.

[93] As discussed earlier, the different terms in the TKE-budget must be parameterized correctly if the inertial dissipation method should work during all conditions. The results in this study show that it is not possible to exclude the transport terms under most conditions, and that the terms are very sensitive to stability, wave age, and wind speed.

8. Discussion

[94] It has been shown that the terms in the TKE-budget depend not just on stability, which has been previously suggested, but also on wave age and to some degree on wind speed. The transport terms are not negligible, not even during neutral conditions. It is mainly the normalized pressure transport term that is responsible for the imbalance. The normalized turbulent transport was found to be very small during all conditions.

[95] The use of the traditional inertial dissipation method (i.e., assuming that the sum of the transport terms is small) therefore seems to be inaccurate during most conditions encountered; correction functions need to be included to account for this imbalance.

[96] The wave age dependence can be divided into three regions, small wave ages ($c_0/(U_{10} \cos\theta) < 0.5$), moderate wave ages with saturated waves $0.5 < c_0/(U_{10} \cos\theta) < 1.2$, and swell $c_0/(U_{10} \cos\theta) > 1.2$.

[97] For small wave ages or high wind speeds, the imbalance between normalized production and normalized dissipation was found to be positive for near neutral conditions (Figure 12). This is in accordance with *Edson and Fairall* [1998], who found that for slightly convective conditions, production exceeded dissipation. Their explanation was that energy is building up the waves rather than being dissipated into heat. Since the waves are growing at these small waves ages, this seems to be the case also here.

[98] For moderate wave ages, we have ''saturated'' conditions, where the waves are neither growing, nor decaying. The sea surface then seems to resemble a land surface, at least in near neutral conditions. The values for the normalized transport terms ($T_tN \approx 0$ and $T_pN \approx 0.25$) and the imbalance between normalized production and normalized dissipation (≈ -0.30), is close to values found over land in similar measurements [e.g., *Högström*, 1996].

[99] For swell dissipation is much larger than production and the normalized pressure transport becomes significant.

[100] The process of ''inactive'' turbulence can probably explain the high values of the pressure transport found during unstable conditions. Inactive turbulence arises in the upper part of the boundary layer and is being brought down to the surface by the pressure transport term. A possible source for inactive turbulence can be a low-level jet at the top of the boundary layer.

[101] This phenomenon is described by *Smedman et al.* [1994]. In that paper an analysis of airborne turbulence measurements throughout a slightly unstable marine boundary layer is presented. It is shown that, in that particular case, ordinary turbulent production at the surface is cut off. Instead, turbulence of boundary layer-size scale was observed to be produced in an elevated shear zone at the top of the boundary layer and brought down to the surface with the aid of the pressure transport mechanism. Although this case with zero turbulence production at the surface is believed to be rather special, the upside-down production mechanism is thought to be at work as soon as there is an elevated shear zone at the top of the boundary layer, a situation which is quite common in the case of a slightly unstable marine boundary layer.

[102] This ''inactive'' part of the turbulence does not contribute to the shearing stress, and does not interact with the ''active'' turbulence. The ''inactive'' turbulence, represented by the pressure transport, is being dissipated at the surface, whereas the production is only the ''active'' turbulence [*Högström*, 1990]. This explains why the dissipation is larger than the production.

[103] Note, however, that as explained by *Högström et al.* [2002], there is an additional process at work during neutral conditions, which will cause downward transport of momentum by the pressure transport term. This mechanism is, however, far from ''inactive,'' being in fact the major agent for momentum transport in the near-neutral surface layer. This process is of surface-layer scale, not of boundary layer scale, as is the inactive turbulence discussed above.

[104] The stress at the surface can be very small during swell conditions (see discussion above), implying that the ''active'' part of the turbulence is small. Only the ''inactive'' part will be left, since this does not contribute to the shearing stress, and energy will be brought down to the surface from higher levels [*Smedman et al.*, 1999] through the pressure transport. Therefore, ''inactive'' turbulence is likely to play an important role during swell conditions.

[105] As discussed by *Rutgersson et al.* [2001], inactive turbulence is not expected to occur during stable conditions. Here instead, the pressure transport term appears to be the result of upward transfer of momentum from the waves during swell, the magnitude of this term decreasing rapidly with height. This contrasts strikingly to the unstable case, which is characterized by observed constancy of T_pN with height, at least up to the highest measuring level, about 26 m

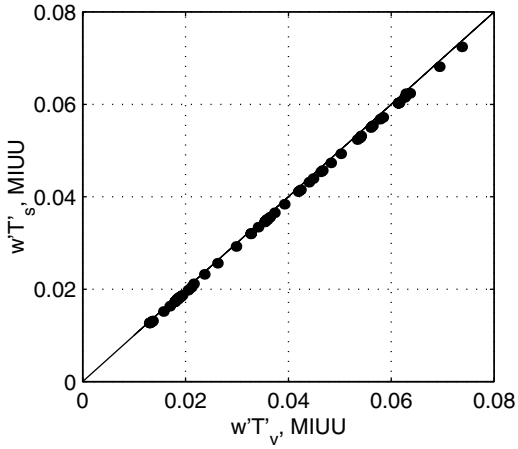

Figure 13. Thirty-minute means of $\overline{w'T'_s}$ plotted against $\overline{w'T'_v}$, both derived from measurements at Östergarnsholm with the MIUU-instrument at 10 m during October, 1999 and computed with (A1) and (A2), respectively.

[*Smedman et al.*, 1999], indicating that energy must also come from above and not only from the waves.

[106] For more convective conditions, however, ϕ_m is very sensitive to the wave conditions, since swell will give negative values for the wind gradient, and therefore negative values of ϕ_m. The normalized buoyancy will also give a significant contribution to the production during unstable conditions. This can be somewhat misleading since, as discussed above, it is mainly u_* that controls the normalized buoyancy, rather than the heat flux, which is usually very small.

[107] As discussed in Section 5.3, the value 0.52 was chosen for the Kolmogorov constant α. This value is based on numerous simultaneous measurements of dissipation and inertial subrange spectra. The analysis shows that for the saturated wave range ($0.5 < c_0/(U_{10} \cos\theta) < 1.2$), it gives results that are in agreement with corresponding results over land. When employing this value of α, however, the transport terms of the TKE-budget become nonzero. As α has been determined in the only physically correct way, this is an inevitable result and a physical reality. The use of an "apparent" Kolmogorov constant is a way to artificially eliminate the effect of the transport term in the TKE-budget, which has been used in some studies, but it is not to be recommended, as we have seen that the magnitude of the transport terms varies considerably with wave age and stability.

9. Conclusions

[108] The main conclusions from this study of the turbulent kinetic energy budget in the marine atmospheric surface layer, where long-term measurements have been used, can by summarized as follows:

1. The imbalance between normalized production and dissipation depends on not only stability, as previously suggested, but also on wave age and to some degree wind speed.

2. Considering the imbalance, the sea surface resembles a land surface for saturated waves ($0.5 < c_0/(U_{10} \cos\theta) < 1.2$) and moderate wind speeds.

3. The normalized dissipation is much larger than the normalized production during swell ($c_0/(U_{10} \cos\theta) > 1.2$) and low wind speeds. Also, the pressure transport term becomes significant and is much larger than the turbulent transport term.

4. Normalized production is larger than normalized dissipation during small wave ages ($c_0/(U_{10} \cos\theta) < 0.5$) and high wind speeds. Contrary to the swell cases, the pressure transport is now negative.

Appendix A. The Relation Between Sonic Temperature Flux and Virtual Temperature Flux

[109] Denoting the fluctuating part of the temperature derived from the sonic signal T_s and the corresponding virtual temperature T_v, the following pair of relations are obtained for the flux of T_s and of T_v, respectively [*Dupuis et al.*, 1997]:

$$\overline{w'T'_S} = \overline{w'T'}(1 + 0.518R) + 0.518\overline{T}\,\overline{w'r'} \qquad \text{(A1)}$$

$$\overline{w'T'_v} = \overline{w'T'}(1 + 0.62R) + 0.62\overline{T}\,\overline{w'r'} \qquad \text{(A2)}$$

[110] Here, $\overline{w'T'}$ is the flux of "ordinary" temperature (K m s^{-1}), R is the mean mixing ratio (kg H_2O/kg dry air), $\overline{T}$ is the mean temperature (K) and $\overline{w'r'}$ the turbulent flux of mixing ratio (m s^{-1}).

[111] Relations (A1) and (A2) were tested on a set of data from Östergarnsholm, when a Solent Ultrasonic anemometer (1210R3, Gill Instrument, Lymington, United Kingdom, referred to as Sonic R3) and a MIUU-instrument were run side by side on 4- and 5-m-long booms, respectively, at the same height, about 10 m above the water surface. The MIUU-instrument [*Högström*, 1982] is basically a wind vane-based three-axial hot-film system supplemented with thin platinum wire sensors for "dry" and "wet bulb" measurements. The test was conducted during October 1999 and the data comprise 54 thirty-minute runs, which

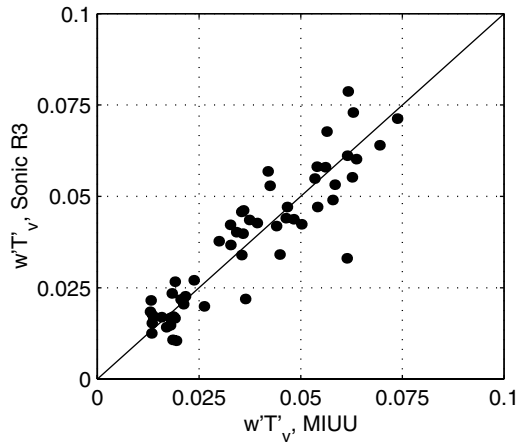

Figure 14. $\overline{w'T'_v}$, measured with the R3 sonic and corrected for the crosswind effect according to *Kaimal and Gaynor* [1991] plotted against the same quantity derived from simultaneous measurements with the MIUU-instrument and obtained with (A2). Same data set as in Figure 13.

include humidity flux measurements with the MIUU-instrument. The situation happened to be fairly representative of autumn conditions at this site, with the sensible heat flux ranging from 15 to 60 W m^{-2} and the corresponding latent heat flux from around 40 to 110 W m^{-2}.

[112] $\overline{w'T'_s}$ and $\overline{w'T'_v}$ were computed with equations (A1) and (A2), respectively, from the temperature flux, $\overline{w'T'}$ and humidity flux, $\overline{w'r'}$ measured with the MIUU-instrument. Figure 13 shows $\overline{w'T'_s}$ plotted against $\overline{w'T'_v}$. In the mean, $\overline{w'T'_v}$ turns out to be about 2% larger than $\overline{w'T'_s}$ for this particular data set. Figure 14 shows the corresponding plot of $\overline{w'T'_v}$ obtained with the Sonic R3 instrument (with cross-wind correction [*Kaimal and Gaynor* [1991]) plotted against $\overline{w'T'_v}$ derived from the simultaneous measurements with the MIUU-instrument. In the mean, the estimates differ by no more than 1%, but the relative scatter is around 20%.

[113] From another intercomparison of 3 MIUU-instruments placed at the same height on a line almost perpendicular to the wind, it was found that the corresponding scatter for the estimate of the heat flux with that type of instrument is about 7%, i.e., about one third of that obtained in the Sonic R3/MIUU-instrument intercomparison. It is concluded that the figure 20% is likely to be typical of the heat flux estimate of a Sonic R3 instrument.

[114] Another intercomparison test at Östergarnsholm with a Solent Ultrasonic anemometer (1012R2, Gill Instrument, Lymington, United Kingdom, referred to as Sonic R2) and a Sonic R3 instrument at the same height (about 10 m) shows that the figure 20% for the uncertainty of the heat flux estimate is likely to be representative as well for the Sonic R2 instrument used in the present study.

[115] As a rather extreme case, consider a situation when the sensible heat flux $\overline{w'T'}$ is zero and the evaporation is as large as 300 W m^{-2}. Making the appropriate conversion, $\overline{w'r'} = 0.1$ and, from (A1), $\overline{w'T'_s} = 14.5$ W m^{-2} and, from (A2), $\overline{w'T'_v} = 17.4$ W m^{-2}, i.e., the difference between the two estimates is no more than 3 W m^{-2}.

[116] From the above analysis, it is clear that the error in the heat flux estimate caused by the difference between sonic temperature and the virtual temperature is quite small in absolute terms as well as in relative terms, 2% of 50 W m^{-2} being only 1 W m^{-2}. For the extreme case of zero sensible heat flux and 300 W m^{-2} latent heat flux, this error will rise to no more than 3 W m^{-2}.

[117] **Acknowledgments.** This work has been performed within the EU-funded project AutoFlux (contract MAS3-CT97-0108). The authors would like to thank Hans Bergström and Mikael Magnusson for help with the data and members of the MIUU staff for participation in the Östergarnsholm field campaigns. Thanks are also given to Ulf Högström for valuable comments on the manuscript. Kimmo Kahma and Heidi Pettersson at FIMR are acknowledged for the wave measurements. Barry Broman at SMHI is acknowledged for the sea level measurements at Visby.

References

Anctil, F., M. A. Donelan, W. M. Drennan, and H. C. Graber, Eddy-correlation measurements of air-sea fluxes from a discus buoy, *J. Atmos. Oceanic. Technol.*, *11*, 1144–1150, 1994.

Anderson, R. J., A study of wind stress and heat flux over the open ocean by the inertial-dissipation method, *J. Phys. Oceanogr.*, *23*, 2153–2161, 1993.

Benilov, A. Y., O. A. Kouznetsov, and G. N. Panin, On the analysis of wind wave-induced disturbances in the atmospheric surface layer, *Boundary Layer Meteorol.*, *6*, 269–285, 1974.

Businger, J. A., J. C. Wyngaard, Y. Izumi, and E. F. Bradley, Flux-profile relationships in the atmospheric surface layer, *J. Atmos. Sci.*, *28*, 181–189, 1971.

Deacon, E. L., The streamwise Kolmogoroff constant, *Boundary Layer Meteorol.*, *42*, 9–17, 1988.

DeCosmo, J., K. B. Katsaros, S. D. Smith, R. J. Anderson, W. A. Oost, K. Bumke, and H. Chadwick, Air-sea exchange of water vapor and sensible heat: The humidity exchange over the sea (HEXOS) results, *J. Geophys. Res.*, *101*, 12,001–12,016, 1996.

Donelan, M. A., W. M. Drennan, and K. B. Katsaros, The air-sea momentum flux in wind sea and swell, *J. Phys. Oceanogr.*, *27*, 2087–2099, 1997.

Drennan, W. M., H. C. Graber, and M. A. Donelan, Evidence for the effects of swell and unsteady winds on marine wind stress, *J. Phys. Oceanogr*, *29*, 1853–1864, 1999a.

Drennan, W. M., K. K. Kahma, and M. A. Donelan, On momentum flux and velocity spectra over waves, *Boundary Layer Meteorol.*, *92*, 489–515, 1999b.

Dupuis, H., A. Weill, K. Katsaros, and P. K. Taylor, Turbulent heat fluxes by profile and inertial dissipation methods: Analysis of the atmospheric surface layer from shipboard measurements during the SOFIA/ASTEX and SEMAPHORE experiments, *Ann. Geophys.*, *13*, 1065–1074, 1995.

Dupuis, H., P. K. Taylor, A. Weill, and K. Katsaros, Inertial dissipation method applied to derive turbulent fluxes over the ocean during the Surface of the Ocean, Fluxes and Interactions with the Atmosphere/Atlantic Stratocumulus Transition Experiment (SOFIA/ASTEX) and Structure des Echanges Mer-Atmosphere, Proprietes des Heterogeneites Oceaniques: Recherche Experimentale (SEMAPHORE) experiments with low to moderate wind speeds, *J. Geophys. Res.*, *102*, 21,115–21,129, 1997.

Edson, J. B., C. W. Fairall, P. G. Mestayer, and S. E. Larsen, A study of the inertial-dissipation method for computing air-sea fluxes, *J. Geophys. Res.*, *96*, 10,689–10,711, 1991.

Edson, J. B., and C. W. Fairall, Similarity relationships in the marine atmospheric surface layer for terms in the TKE and scalar variance budgets, *J. Atmos. Sci.*, *55*, 2311–2328, 1998.

Fairall, C. W., and S. E. Larsen, Inertial-dissipation methods and turbulent fluxes at the air-ocean interface, *Boundary Layer Meteorol.*, *34*, 287–301, 1986.

Fairall, C. W., J. B. Edson, S. E. Larsen, and P. G. Mestayer, Inertial-dissipation air-sea flux measurements: A prototype system using real time spectral computations, *J. Atmos. Oceanic. Technol.*, *7*, 425–453, 1990.

Geernaert, G. L., F. Hansen, M. Courtney, and T. Herbers, Directional attributes of the ocean surface wind stress vector, *J. Geophys. Res.*, *98*, 16,571–16,582, 1993.

Grachev, A. A., and C. W. Fairall, Upward momentum transfer in the marine boundary layer, *J. Phys. Oceanogr.*, *31*, 1698–1711, 2001.

Grelle, A., and A. Lindroth, Flow distortion by a Solent sonic anemometer: Wind tunnel calibration and its assessment for flux measurements over forest and field, *J. Atmos. Oceanic Technol.*, *11*, 1529–1542, 1994.

Hicks, B. B., and A. J. Dyer, The spectral density technique for the determination of eddy fluxes, *Quart. J. R. Met. Soc.*, *98*, 838–844, 1972.

Högström, U., A critical evaluation of the aerodynamical error of a turbulence instrument, *J. Appl. Meteorol.*, *21*, 1838–1844, 1982.

Högström, U., Von Kármán's constant in atmospheric boundary layer flow: Reevaluated, *J. Atmos. Sci.*, *42*, 263–270, 1985.

Högström, U., Non-dimensional wind and temperature profiles in the atmospheric surface layer: A re-evaluation, *Boundary Layer Meteorol.*, *42*, 55–78, 1987.

Högström, U., Analysis of turbulence structure in the surface layer with a modified similarity formulation for near neutral conditions, *J. Atmos. Sci.*, *47*, 1949–1972, 1990.

Högström, U., Review of some basic characteristics of the atmospheric surface layer, *Boundary Layer Meteorol.*, *78*, 215–246, 1996.

Högström, U., J. C. R. Hunt, and A. Smedman, Theory and measurements for turbulence spectra and variances in the atmospheric neutral surface layer, *Boundary Layer Meteorol.*, *103*, 124–191, 2002.

Janssen, P. A. E. M., On the effect of ocean waves on the kinetic energy balance and consequences for the inertial dissipation method, *J. Phys. Oceanogr.*, *29*, 530–534, 1999.

Kaimal, J. C., and J. E. Gaynor, Another look at sonic thermometry, *Boundary Layer Meteorol.*, *56*, 401–410, 1991.

Katsaros, K. B., S. D. Smith, and W. A. Oost, HEXOS-Humidity Exchange Over the Sea, a program for research on water-vapor and droplet fluxes from sea to air at moderate to high wind speeds, *Bull. Am. Meteorol. Soc.*, *68*, 466–476, 1987.

Kitaigorodskii, S. A., *The Physics of Air-Sea Interaction*, Engl. Transl., 237 pp., Israel Prog. for Sci. Transl., Jerusalem, Israel, 1973.

Large, W. G., and S. Pond, Open ocean momentum flux measurements in moderate to strong winds, *J. Phys. Oceanogr.*, *11*, 324–336, 1981.

Large, W. G., and S. Pond, Sensible and latent heat flux measurements over the ocean, *J. Phys. Oceanogr.*, *12*, 464–482, 1982.

Makova, V. I., Features of the dynamics of turbulence in the marine atmospheric surface layer at various stages in the development of waves, *Izv. Russ. Acad. Sci. Atmos. Oceanic Phys., Engl. Transl.*, *11*, 177–182, 1975.

Miyake, M., R. W. Stuart, and R. W. Burling, Spectra and cospectra of turbulence over water, *Q. J. R. Meteorol. Soc.*, *96*, 138–143, 1970.

Pierson, W. J., Jr., and L. Moskowitz, A proposed spectral form for fully developed wind seas based on the similarity theory of S. A. Kitaigorodskii, *J. Geophys. Res.*, *69*, 5181–5190, 1964.

Rieder, K. F., and J. A. Smith, Removing wave effects from the wind stress vector, *J. Geophys. Res.*, *103*, 1363–1374, 1998.

Rutgersson, A., A. Smedman, and U. Högström, The use of conventional stability parameters during swell, *J. Geophys. Res.*, *106*, 27,117–27,134, 2001.

Schacher, G. E., K. L. Davidson, T. Houlihan, and C. W. Fairall, Measurements of the rate of dissipation of turbulent kinetic energy, ε, over the ocean, *Boundary Layer Meteorol.*, *20*, 321–330, 1981.

Schotanus, P., F. T. M. Nieuwstadt, and H. A. R. DeBruin, Temperature measurements with a sonic anemometer and its application to heat and moisture fluxes, *Boundary Layer Meteorol.*, *26*, 81–93, 1983.

Smedman, A., M. Tjernström, and U. Högström, The near-neutral marine atmospheric boundary layer with no surface shearing stress: A case study, *J. Atmos. Sci.*, *51*, 3399–3411, 1994.

Smedman, A., U. Högström, H. Bergström, A. Rutgersson, K. K. Kahma, and H. Pettersson, A case study of air-sea interaction during swell conditions, *J. Geophys. Res.*, *104*, 25,833–25,851, 1999.

Smith, S. D., et al., Sea surface wind stress and drag coefficients: The HEXOS results, *Boundary Layer Meteorol.*, *60*, 109–142, 1992.

Smith, S. D., C. W. Fairall, G. L. Geernaert, and L. Hasse, Air-sea fluxes: 25 years of progress, *Boundary Layer Meteorol.*, *78*, 247–290, 1996.

Stull, R. B., *An Introduction to Boundary Layer Meteorology*, 666 pp., Kluwer Acad., Norwell, Mass., 1988.

Taylor, P. K., and M. J. Yelland, Comments on: On the effect of ocean waves on the kinetic energy balance and consequences for the inertial dissipation technique, *J. Phys. Oceanogr.*, *31*, 2532–2536, 2001.

Tennekes, H., The logarithmic wind profile, *J. Atmos. Sci.*, *30*, 234–238, 1973.

Volkov, Y. A., Turbulent flux of momentum and heat in the atmospheric surface layer over a disturbed sea-surface, *Izv. Russ. Acad. Sci. Atmos. Oceanic Phys., Engl. Transl.*, *6*, 770–774, 1970.

Wilczak, J. M., J. B. Edson, J. Hojstrup, and T. Hara, The turbulent kinetic energy in the marine atmospheric surface layer, in *Air-Sea Exchange: Physics, Chemistry and Dynamics*, edited by G. L. Geernaert, pp. 153–173, Kluwer Acad., Norwell, Mass., 1999.

Wyngaard, J. C., and O. R. Coté, The budgets of turbulent kinetic energy and temperature variance in the atmospheric surface layer, *J. Atmos. Sci.*, *28*, 190–201, 1971.

Yelland, M., and P. K. Taylor, Wind stress measurements from the open ocean, *J. Phys. Oceanogr.*, *26*, 541–558, 1996.

A. Sjöblom and A. Smedman, Department of Earth Sciences, Meteorology, Uppsala University, Geocentrum Villav. 16, SE-752 36, Uppsala, Sweden. (Anna.Sjoblom@met.uu.se)